Sonoluminescence

The Origin of Isotope Effects in Sonoluminescence Spectra of Heavy and Light Water**

Abdoul Aziz Ndiaye, Rachel Pflieger, Bertrand Siboulet, and Sergey I. Nikitenko

The production of hydroxyl radicals in water under power ultrasound plays a central role in a wide range of sonochemical advanced oxidation processes.[1] Thorough analysis of sonoluminescence (SL) spectra is a powerful tool to understand the origin of the drastic conditions created by acoustic cavitation that lead to water-molecule splitting. Recent studies of SL from water under power ultrasound revealed the overpopulation of $OH(A^2\Sigma^+)$ vibrational levels indicating non-equilibrium plasma formation inside the collapsing bubbles.[2] This finding correlates with the Treanor kinetic isotope effect reported for carbon monoxide disproportionation in aqueous solutions driven by power ultrasound.[3] To date, there is only limited information about the isotope effects in SL spectra. Hiller and Putterman reported a dramatic effect of heavy water on single bubble sonoluminescence (SBSL) in the presence of H_2 and D_2.[4] They found that heavy water importantly shifted the whole SBSL spectrum towards red wavelengths. Lepoint et al. observed a small blue wavelength shift for $OH/OD(A^2\Sigma^+-X^2\Pi_i)$ (0,0), (1,1), and (2,2) vibronic transitions in argon-saturated D_2O under 20 kHz ultrasound compared to the OH(A-X) system under similar conditions.[5] They also reported modifications in the spectral shape of the OH(A-X) system in D_2O. Nevertheless, the isotope effects in SL spectra have not yet found a reasonable explanation. Herein, we report for the first time multi-bubble sonoluminescence (MBSL) spectra obtained in light and heavy water saturated with Ar or Xe noble gases at various ultrasonic frequencies. The detailed spectroscopic analysis of $OH/OD(A^2\Sigma^+-X^2\Pi_i)$ emission bands reveals the isotope effects in MBSL spectra can be explained by the formation of plasma with non-equilibrium vibrational excitation of $OH^\bullet/OD^\bullet$ radicals.

Figure 1 shows typical SL spectra of H_2O and D_2O, saturated with Ar or Xe, and obtained at 20 kHz and 1057 kHz ultrasound. The results at other frequencies are shown in Figure S2 e–j of the Supporting Information. Despite the very small variation in physico-chemical properties of H_2O and D_2O, their SL spectra exhibit a striking difference whatever the ultrasonic frequency or the saturating noble gas. The $OH/OD(A^2\Sigma^+-X^2\Pi_i)$ emission bands in the

wavelength interval 270–360 nm exhibit not only the isotope shift because of the slightly different vibrational transition wavelengths for OH and OD but also spectral profile modifications indicating differences in the populations of the $OH/OD(A^2\Sigma^+)$ vibrational levels. Surprisingly, the strong emission from the $OH(C^2\Sigma^+)$ excited state observed in light water at $\lambda < 270$ nm[7] is dramatically reduced in heavy water.

To elucidate the origin of the observed isotope effects, the vibrational populations of $OH/OD(A^2\Sigma^+)$ electronic states were calculated using the methodological approach for SL spectra analysis developed by us.[2] In brief, the SL spectra were deconvoluted after baseline subtraction presuming a Gaussian distribution of the vibrational emission bands. The wavelengths of $OH/OD(A^2\Sigma^+-X^2\Pi_i)$ transitions were optimized referring to those given in Lifbase database[8] (Table S1–S4 in the Supporting Information) until best fits were achieved between the SL experimental spectra and the deconvoluted ones. The results of deconvoluted SL spectra are shown in Figures S3–S6.

Then the populations of the $OH/OD(A^2\Sigma^+)$ vibrational states (N_ν^r) from N_1 up to N_4 relative to N_0 were calculated from the established equation for an optically thin plasma[9] using intensity ratios of the deconvoluted molecular bands. Radiative transition probabilities $A_{\nu'\nu''}$ and Klein–Dunham constants were taken from Lifbase[8] and the work of Luque and Crosley[9] respectively (Tables S5, S7, and S10). Figure 2 shows the relative vibrational population distribution of the $OH/OD(A^2\Sigma^+)$ states as a function of vibrational energy for low (20 kHz) and high (1057 kHz) ultrasound frequencies. The N_ν^r values for other frequencies are listed in Table S6. The distribution of the relative populations N_ν^r plotted in Figure 2 and Figure S10 clearly indicates overpopulation of $OH^\bullet$ and $OD^\bullet$ vibrational levels compared to Boltzmann equilibrium distribution in the whole range of studied conditions. Note that the N_1 values for both $OH^\bullet$ and $OD^\bullet$ species in ultrasonic plasma (Table S6) are more than twice those reported in plasma produced by electron impact on H_2O and D_2O in a supersonic free jet.[11]

In Figure 3, the isotope effect for relative $OD/OH(A^2\Sigma^+)$ vibrational populations $\left(\alpha = \frac{N_\nu^{OD}}{N_\nu^{OH}}\right)$ is plotted against the energy difference $\left(\Delta E = (\Delta E_\nu^{OH} - \Delta E_\nu^{OD})\right)$ for the corresponding vibrational levels. For comparison, Figure 3 also presents Lifbase simulation for thermalized $OD/OH(A^2\Sigma^+)$ systems at $T_0 = 5000$ K which is taken as the intra-bubble gas temperature during multi-bubble cavitation in water presuming adiabatic collapse.[12]

From Figure 3 it is clear that whatever the ultrasonic frequency and the rare gas, $\ln\alpha$ does not follow an exponential Boltzmann function. In argon, $\ln\alpha$ slightly decreases with ΔE

[*] Dr. A. A. Ndiaye, Dr. R. Pflieger, Dr. B. Siboulet, Dr. S. I. Nikitenko
Institute for Separation Chemistry of Marcoule (ICSM)
UMR 5257, CEA-CNRS-UMII-ENSCM
BP 17171, 30207 Bagnols-sur-Cèze, Cedex (France)
E-mail: serguei.nikitenko@cea.fr

Supporting information for this article is available on the WWW under http://dx.doi.org/10.1002/anie.201208891.
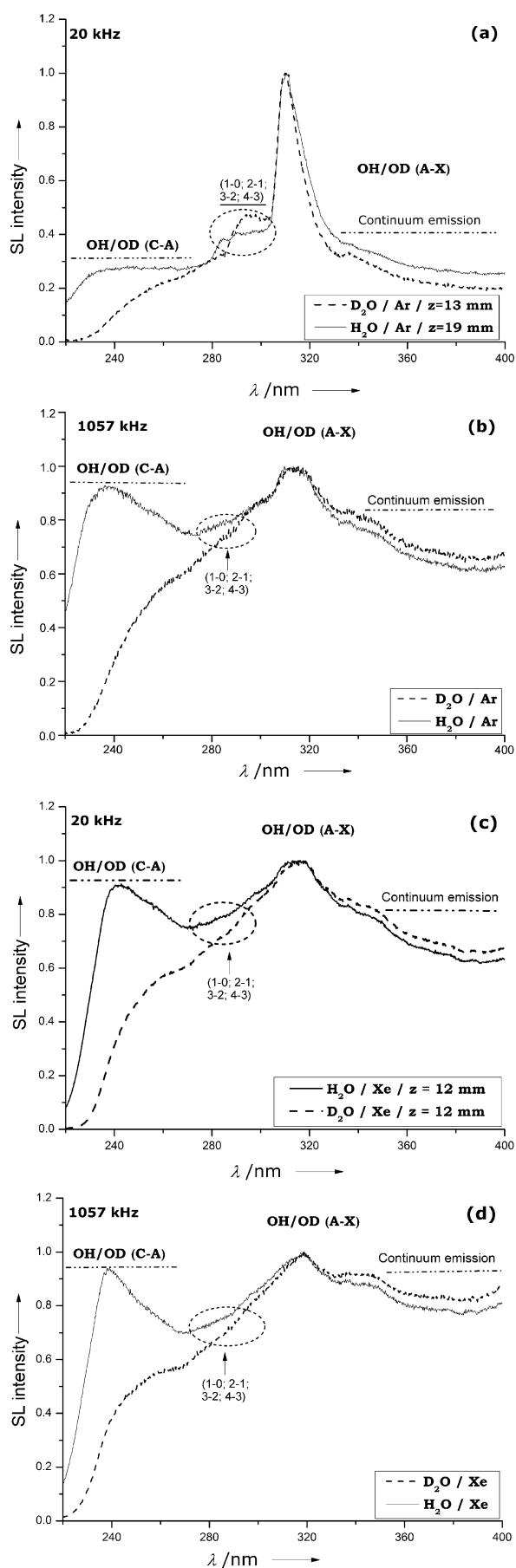
except for the curve at 20 kHz which exhibits a minimum at $v_i = 3$. This striking feature may be related to different excitation regimes for OH· and OD· species at these conditions. Figure 2a shows that at 20 kHz the hyperbolic distribution function of OH($A^2\Sigma^+$) fits with a weak Brau vibrational excitation.[2,10] In contrast, the population of the OD($A^2\Sigma^+$) vibrational levels follows a strongly excited exponentially parabolic Treanor distribution under similar conditions. In both cases the population of excited vibrational levels occurs through an anharmonic vibration-to-vibration pumping (V–V) mechanism. However, the strong excitation regime requires vibrational temperatures exceeding 5000 K.[10] In contrast, weak excitation means lower vibrational temperatures which implies that the V–V exchange for OH· and OD· radicals at 20 kHz in argon is described by different distribution functions. In contrast, at high-frequency ultrasound the distribution functions shown in Figure 2a reveal strong vibrational excitation for both species.

In Xe, the vibrational population distribution for OH· and OD· radicals (Figure 2b) exhibits Treanor behavior for the whole range of ultrasonic frequencies studied. The decrease of $\ln\alpha$ with ΔE in Xe is even more pronounced than that in Ar (Figure 3). Moreover, in both gases, the $\ln\alpha$ values for $v_i \geq 2$ are below those calculated at thermal equilibrium ($T_0 = 5000$ K). The striking decrease of $\ln\alpha$ is related to the contribution of vibrational–translational (V–T) relaxation process which competes with V–V pumping.[10] According to the Landau–Teller formula, the V–T relaxation rate is related to translational gas temperature (T_0) as $\exp\left(-\frac{B}{T_0^{1/3}}\right)$. Consequently, the Treanor isotope effect decreases with T_0: the higher the gas temperature, the higher the probability of V–T relaxation and consequently of depletion of the higher vibrational levels.[13] Hence the trend followed by $\ln\alpha$ can be explained by formation of a "hotter" plasma in D_2O than in H_2O. Note that the vapor pressure of H_2O is about 20% higher at 10°C than that of D_2O[14] which could explain higher T_0 value in heavy water.

Actually, a non-equilibrium plasma is characterized not only by T_0 but also by electron (T_e), vibrational (T_v), and rotational (T_r) temperatures which significantly differ from each other: $T_e > T_v > T_r \approx T_0$.[10] The T_e and T_v values calculated using our procedure of SL spectra simulation[2] are summarized in Table 1. The selected spectroscopic data incorporated in the SL simulated spectra for the OD(A-X) system are presented (Tables S7–S11, Figure S7–S9). For the OH(A-X) band transitions, the spectroscopic data are reported in our previous work.[2] The vibronic temperatures obtained are higher in D_2O than in H_2O confirming the hypothesis of a "hotter" plasma in heavy water.

Figure 1. SL spectra normalized to OH/OD($A^2\Sigma^+ - X^2\Pi_i$) (0-0) transitions in H_2O and D_2O at $T = 10$–11°C: a) $f = 20$ kHz, $P_{ac} = 30$ W, Ar, z is the axial position with the highest SL intensity;[6] b) $f = 1057$ kHz, $P_{ac} = 85$ W, Ar; c) $f = 20$ kHz, $P_{ac} = 30$ W, Xe; d) $f = 1057$ kHz, $P_{ac} = 82$ W, Xe. The emission band at $\lambda \approx 336$ nm in Figure 1a originates from the N_2 [C $^3\Pi_u$ ($v' = 0$)→B $^3\Pi_g$ ($v'' = 0$)] transition arising from the presence of traces of air. In general, the total SL intensity in Xe is three- to fourfold higher than that in Ar.
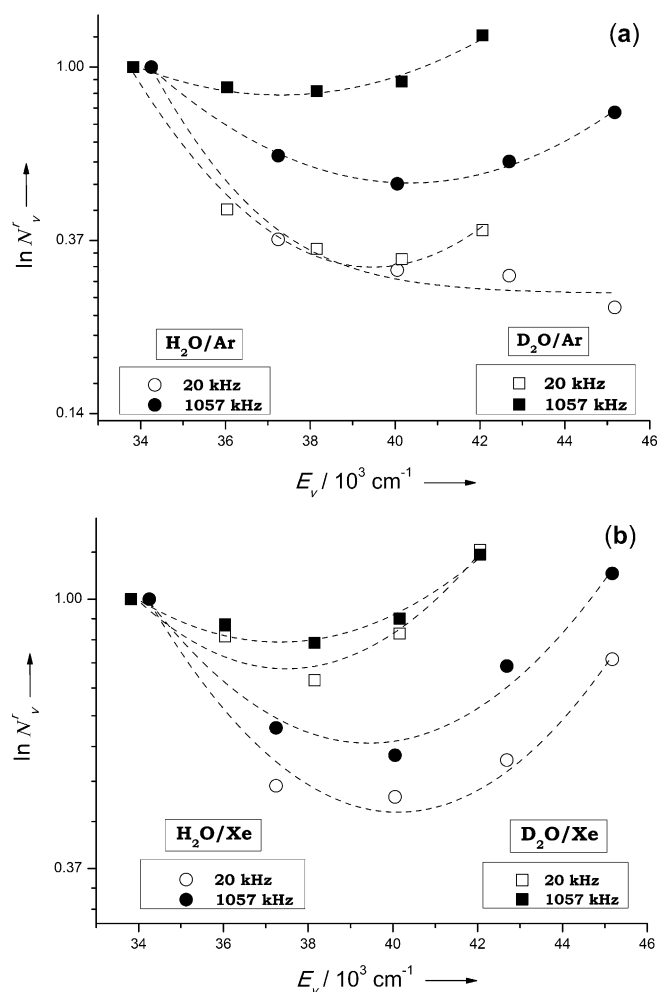
Figure 2. Relative vibrational population distribution of the OH/OD-(A$^2\Sigma^+$) states as a function of vibrational energy for 20 kHz and 1057 kHz in the presence of Ar (a) and Xe (b). Data for the H$_2$O/Ar system are taken from Ref [2]. The observed shift along the *x*-axis between the OH$^\bullet$ and OD$^\bullet$ curves is due to the lower vibrational-energy values for OD$^\bullet$.[10]

Figure 3. Variation of lnα with the vibrational-energy differences for OH/OD (A$^2\Sigma^+$–X$^2\Pi_i$) (v_i = 1–4) transitions in the presence of Ar (a) and Xe (b) and comparison with OH/OD(A$^2\Sigma^+$) thermalized systems calculated with Lifbase at T_0 = 5000 K. The absolute uncertainty for experimental lnα values is estimated to approximately 20%.

The higher T_e and T_v values in Xe than Ar are a result of the lower ionization potential of Xe (12.13 eV for Xe, 15.76 eV for Ar).[15] The ultrasonic frequency has a relatively small effect on the vibronic temperatures in heavy water saturated with Xe gas indicating that in this case the electron density inside the collapsing bubble is driven more by the Xe ionization potential than by bubble collapse itself. Note that the much greater total SL intensity in Xe (Figure 1) can be explained not only by higher vibronic temperatures but also by a larger number of active bubbles resulting from the higher Xe solubility.[16]

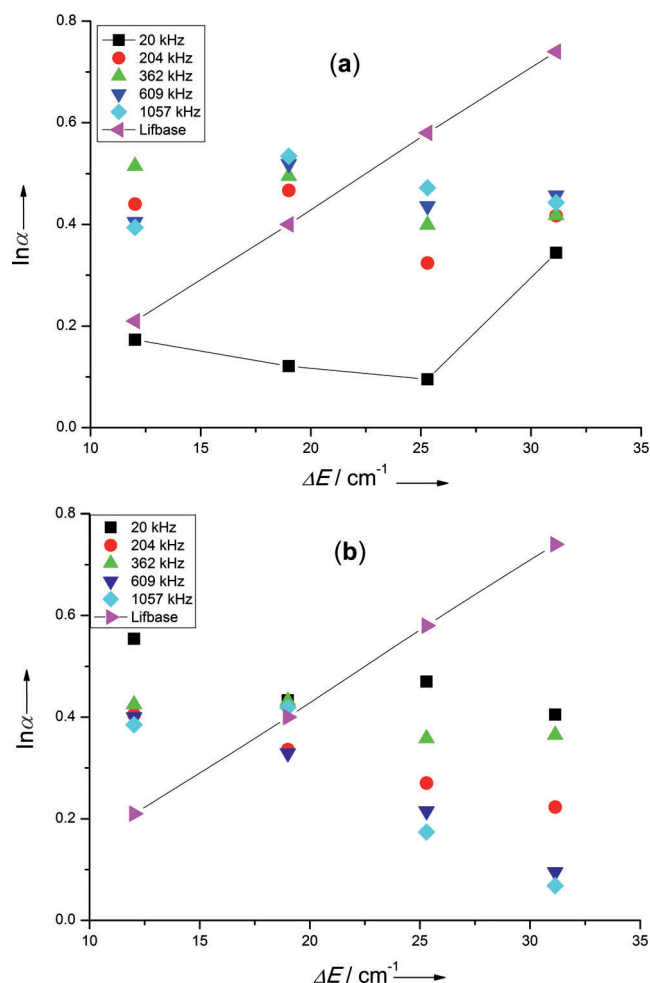The sharp decrease in the C$^2\Sigma^+$–A$^2\Sigma^+$ emission band intensities in heavy water compared to those in light water (Figure S1 and Figure S2) is probably related to the different vibrational-band transitions observed for OH$^\bullet$ and OD$^\bullet$ in a non-equilibrium plasma at 240–270 nm. The OH/OD(C$^2\Sigma^+$–A$^2\Sigma^+$) emission extends from the far ultraviolet to about 270 nm.[17] The low-level transitions of the OH/OD(C-A) systems at λ < 230 nm are not visible in our

Table 1: Calculated values of electron (T_e) and vibrational (T_v) temperatures for H$_2$O and D$_2$O as a function of gas and ultrasonic frequency.[a]

Frequency [kHz]	H$_2$O/Ar[b]		D$_2$O/Ar		H$_2$O/Xe		D$_2$O/Xe	
	T_v [K]	T_e [K]	T_v [K]	T_e [K]	T_v [K]	T_e [K]	T_v [K]	T_e [K]
20	5000	8000	5900	8800	7900	9900	9570	11370
204	7600	9500	8200	9900	7650	9300	8380	11000
362	8450	10000	9200	10950	8500	10800	9400	11200
609	9050	11000	10060	11400	9850	11900	9610	12200
1057	9800	12000	10850	12200	10700	12800	10120	13500

[a] The temperature in the reactor during sonolysis is maintained at T = 10–11 °C. The uncertainty in vibronic-temperature determination is estimated to be 15–20%. The T_0 (T_r) values cannot be assessed from our SL spectra because their rotational structure is not resolved. [b] Data from Ref. [2].

experiments because of the absorption by water and the lack of sensitivity of the grating in this spectral range. At 230–260 nm the OH($C^2\Sigma^+ - A^2\Sigma^+$) system exhibits numerous overlapping emission bands such as 0-ν''(6–9), 1-ν''(7–9), and (3,7) while the OD($C^2\Sigma^+ - A^2\Sigma^+$) system shows only few 0-ν''(11;12) bands in this spectral range.[18,19] Consequently, the intensity of OD(C-A) emission bands in water is much lower than that of OH(C-A). Besides, it can be suggested that in a sonochemical plasma the higher vibrational states are quenched more effectively in heavy water that in light water via a V–T relaxation mechanism. Note that the OH/OD(C-A) transitions in the spectral range studied could be overlapping with (4-1), (2-0), and (3-1) transitions of OH/OD(A-X).[18] Therefore, the interpretation of the effects related to the OH/OD(C-A) emission bands needs to be treated with some caution.

In summary, the isotope effects reported show unequivocally that the generation of OH· radicals during water sonolysis should be considered as a non-equilibrium plasma chemical process rather than an adiabatic heating flame-like process. Moreover, the non-equilibrium model can contribute to an understanding of the cavitation mechanisms, not only in water, but also in other media. For instance, the spectroscopic study of SBSL in sulfuric acid in the presence of noble gases revealed emission lines from Xe^+, Kr^+, and Ar^+ with the energies ranging from 26.0 eV to 34.2 eV.[20] However, the gas temperature obtained at the same conditions is only about 1 eV (ca. 10000 K).[21] Such a discrepancy cannot be understood by presuming only adiabatic heating during bubble collapse, but it can be explained by the formation of a non-equilibrium plasma with an electron temperature higher than the gas temperature. Thus it can be concluded that a non-equilibrium plasma is the major state of gas inside violently collapsing cavitation bubbles.

Experimental Section

The experiments were performed using a multifrequency ultrasonic device operated at 20, 204, 362, 609, and 1057 kHz. Deionized light water (18.2 MΩ cm^{-1}) and heavy water (EURISO-TOP, 99.90 % D) were continuously sparged with pure Ar or Xe at 100 mL min^{-1} 30 min before and during ultrasonic treatment. The temperature in the reactor during sonolysis was maintained at 10–11 °C. The absorbed acoustic power was measured by a conventional thermal probe method.[22] The SL spectra were collected in the spectral range 200 nm to 400 nm using a SP 2356i Roper Scientific spectrometer (grating 300 gr mm^{-1} blazed at 300 nm, focal length 300 nm, f/3.9 in aperture ratio, slit width 0.1 mm, resolution better than 1.5 nm) coupled to SPEC10–100BR CCD camera with UV coating (Roper Scientific) cooled by liquid nitrogen. Further experimental details are in the Supporting Information. The numerical deconvolution of SL spectra was performed using Wolfram Mathematica 7 software. The procedures for SL emission spectra deconvolution, determination of the vibrational population distribution, and the vibronic temperatures (T_v, T_e) calculation are described in the Supporting Information.

[1] Y. G. Adewuyi, *Ind. Eng. Chem. Res.* **2001**, *40*, 4681–4715.
[2] A. A. Ndiaye, R. Pflieger, B. Siboulet, J. Molina, J.-F. Dufrêche, S. I. Nikitenko, *J. Phys. Chem. A* **2012**, *116*, 4860–4867.
[3] S. I. Nikitenko, P. Martinez, T. Chave, I. Billy, *Angew. Chem.* **2009**, *121*, 9693–9696; *Angew. Chem. Int. Ed.* **2009**, *48*, 9529–9532.
[4] R. A. Hiller, S. J. Putterman, *Phys. Rev. Lett.* **1995**, *75*, 3549–3551.
[5] T. Lepoint, F. Lepoint-Mullie, N. Voglet, S. Labouret, C. Pétrier, R. Avni, J. Luque, *Ultrason. Sonochem.* **2003**, *10*, 167–174.
[6] In D$_2$O, the strongest SL is observed at longer axial distance from the ultrasonic horn than in H$_2$O under similar conditions. The origin of this striking phenomenon is not clear and should be the subject of further study.
[7] R. Pflieger, H.-P. Brau, S. I. Nikitenko, *Chem. Eur. J.* **2010**, *16*, 11801–11803.
[8] J. Luque, D. R. Crosley, LIFBASE: Database and Spectral Simulation Program (Version 1.5), **1999**, SRI Int. Rep. MP 99-009 (http://www.sri.com/cem/lifbase).
[9] J. Luque, D. Crosley, *J. Chem. Phys.* **1998**, *109*, 439–445.
[10] A. Fridman, *Plasma Chemistry.* Cambridge University Press, Cambridge, **2008**.
[11] K. Furuya, F. Koba, T. Ogawa, *Spectrochim. Acta Part A* **1997**, *53*, 665–669.
[12] a) Y. T. Didenko, W. B. McNamara III, K. S. Suslick, *J. Am. Chem. Soc.* **1999**, *121*, 5817–5818; b) E. Ciawi, J. Rae, M. Ashokkumar, F. Grieser, *J. Phys. Chem. B* **2006**, *110*, 13656–13660.
[13] "Isotope Separation by Vibration–Vibration Pumping": J. W. Rich, R. C. Bergman, *Nonequilibrium Vibrational Kinetics, Topics in Current Physics, Vol. 39* (Ed.: M. Capitelli), Springer, Berlin, **1986**, pp. 271–293.
[14] N. Matsunaga, A. Nagashima, *Int. J. Thermophys.* **1987**, *8*, 681–694.
[15] E. Well, J. M. DeWitt, R. R. Jones, *Phys. Rev. A* **2002**, *66*, 013409.
[16] C. Browne, R. F. Tabor, D. Y. C. Chan, R. R. Dagastine, M. Ashokkumar, F. Grieser, *Langmuir* **2011**, *27*, 12025–12032.
[17] T. I. Quickenden, J. A. Irvin, *J. Chem. Phys.* **1978**, *69*, 4395–4402.
[18] C. Carlone, F. W. Dalby, *Can. J. Phys.* **1969**, *47*, 1945–1957.
[19] P. Felenbok, *Ann. Astrophys.* **1963**, *26*, 393–428.
[20] D. J. Flannigan, K. S. Suslick, *Phys. Rev. Lett.* **2005**, *95*, 044301.
[21] D. J. Flannigan, K. S. Suslick, *Nat. Phys.* **2010**, *6*, 598–601.
[22] N. M. Navarro, T. Chave, P. Pochon, I. Bisel, S. I. Nikitenko, *J. Phys. Chem. B* **2011**, *115*, 2024–2029.